




Total-body PET/CT using half-dose FDG and compared with conventional PET/CT using full-dose FDG in lung cancer

Hui Tan^{1,2,3} · Xiuli Sui^{1,2,3} · Hongyan Yin^{1,2,3} · Haojun Yu^{1,2,3} · Yusen Gu^{1,2,3} · Shuguang Chen^{1,2,3} · Pengcheng Hu^{1,2,3} · Wujian Mao^{1,2,3} · Hongcheng Shi^{1,2,3} 

Received: 4 May 2020 / Accepted: 26 October 2020 / Published online: 27 November 2020
© Springer-Verlag GmbH Germany, part of Springer Nature 2020

Abstract

Purpose The purpose was to explore the effects of total-body PET/CT with half-dose ¹⁸F-FDG activity on image quality, compared with those of conventional PET/CT with clinical routine full-dose ¹⁸F-FDG in lung cancer.

Methods Fifty-six primary lung cancer patients who underwent total-body PET/CT on a uEXPLORER scanner with half-dose (1.85 MBq/kg) ¹⁸F-FDG activity before treatment were retrospectively studied; among them, 28 patients were confirmed by postoperative pathologic examination and 28 patients by biopsy. After matching with the pathological study results, the other 28 patients with lung cancer who underwent surgery were selected for the full-dose (3.70 MBq/kg) group. Patients in the full-dose group were studied with a conventional uM780 PET/CT scanner. The acquisition time of the half-dose group was 15 min, split into 4-min and 2-min duration groups, which were all referred to as G15, G4 and G2, respectively. The PET/CT scanning speed in the full-dose group was 2 min/bed. Image quality was evaluated by subjective and objective analyses. The subjective analysis method was carried out with a 5-point scale (5-excellent, 1-poor). Objective analysis indicators of PET image quality included the SUVmax, SUVmean and signal-to-noise ratio (SNR) of the liver; the SUVmax and SUVmean of the blood pool; and the SUVmax and tumour-to-background ratio (TBR) of the lesions. G15 served as the reference for G2 and G4 to test lesion detectability.

Results Image quality scores in G2 (4.3 ± 0.7) were significantly higher than those in the full-dose group (3.7 ± 0.6) ($p = 0.004$). The mean and SD of the image quality scores in G4 and G15 were 4.9 ± 0.2 and 5.0 ± 0.0, respectively. The liver SNR in G2 was significantly higher than that in the full-dose group; the corresponding SNR were 11.7 ± 1.5 and 8.3 ± 1.2 ($p < 0.001$), respectively. The liver SNR significantly increased with the time of acquisition among G2, G4 and G15 (11.1 ± 1.7, 15.2 ± 3.4 and 30.5 ± 6.0, all $p < 0.05$). G15 served as the reference, and all these lesions (100%) could be identified by G2 and G4.

Conclusion Total-body PET/CT with half-dose ¹⁸F-FDG activity in G2 and G4 achieved comparable image quality to conventional PET/CT, and its image quality was better than that of conventional PET/CT with clinical routine full-dose ¹⁸F-FDG in lung cancer.

Keywords Half-dose · Full-dose · Total-body · PET/CT imaging · Lung cancer

Hui Tan and Xiuli Sui contributed equally to this work.

This article is part of the Topical Collection on Oncology - Chest

✉ Hongcheng Shi
shi.hongcheng@zs-hospital.sh.cn

¹ Department of Nuclear Medicine, Zhongshan Hospital, Fudan University, 180 Fenglin Road, Shanghai 200032, China

² Nuclear Medicine Institute of Fudan University, Shanghai 200032, China

³ Shanghai Institute of Medical Imaging, Shanghai 200032, China

Introduction

Positron emission tomography/computed Tomography (PET/CT) with F-18-fluorodeoxyglucose (¹⁸F-FDG) plays an important role in tumour diagnosis, staging, restaging, efficacy evaluation, etc., and guides the selection of clinical treatment options [1–5]. The performance of PET depends on the scintillator used in the detector. NaI (Tl) was the first fast scintillator with high light yield that could provide good resolution and was commonly used in the mid-1970s. Nevertheless, low density and effective atomic number resulted in limited sensitivity. Therefore, the bismuth germanite (BGO) scintillator,

which has a high density and atomic number, was selected as a substitution [6]. With the development of scintillator material, lutetium oxyorthosilicate (LSO) was discovered to have a higher density and a faster decay time than BGO. Currently, LSO-based PET has become the dominant PET detection material and can provide a good resolution with a short scan time.

There are two main factors that result in the poor sensitivity of current whole-body PET scans [7]. First, approximately 85–90% of the body is outside the axial field of view (FOV) of the scanner. Second, even within the FOV of the scanner, hardly any available signals can be collected. Compared with whole-body PET scanners, total-body PET scanners have demonstrated great improvements: total-body PET/CT scanners are equipped with LYSO crystal and silicon photomultiplier (SiPM) photoelectric conversion technology with the application of an optimal algorithm, possessing a 194-cm-long FOV that allows the simultaneous recording of coincidence photons from the entire human body, and the sensitivity can be increased by a factor of approximately 40-fold [7–9]. With these improvements in the performance of clinical PET/CT equipment, total-body PET scanners can achieve comparable image quality with a significant reduction in tracer activity [9]. In clinical practice, the injected activity is often restricted by concerns about the radiation dose to patients. However, to the best of our knowledge, there have been few studies about PET/CT with low-dose injection activity. Our preliminary clinical case showed that in a subject weighing 43.5 kg after the injection of 25 MBq (0.58 MBq/kg) ^{18}F -FDG and waiting for 50 min with subsequent data acquisition for 10 min by a total-body PET scan, the image quality met the diagnostic needs [9]. Therefore, our team aimed to explore whether reducing ^{18}F -FDG injection activity could meet the needs of clinical diagnosis. The study showed the image quality and diagnostic efficacy of total-body PET/CT imaging with 1.85 MBq/kg ^{18}F -FDG in lung cancer and compared it with that of conventional PET/CT imaging with clinically routine 3.7 MBq/kg ^{18}F -FDG.

Materials and methods

Patients

In this study, we retrospectively collected data from fifty-six primary lung cancer patients who underwent total-body PET/CT with half-dose (1.85 MBq/kg) ^{18}F -FDG activity before treatment. Of them, 28 patients (30 lesions) received surgical treatment, and the others received endobronchial ultrasound with real time-guided transbronchial needle aspiration (EBUS-TBNA). All of them were diagnosed with primary lung cancer confirmed by pathological study. All scans were performed and evaluated by Zhongshan Hospital Fudan University between October 2019 and May 2020. Patients

were excluded if there were no avid FDG findings in lung cancer. The characteristics of the patients were summarized in Table 1.

After matching with the pathological results, another 28 lung cancer patients (30 lesions) who underwent surgery were selected for the full-dose (3.70 MBq/kg) group. Patients in the full-dose group were studied with a conventional uM780 PET/CT scanner, and their imaging quality was compared with that of total-body PET/CT with half-dose ^{18}F -FDG activity. These patients with lung cancer had avid FDG findings. To minimize the impact on PET/CT image quality, we matched and screened the two groups. The preliminary preparation and inspection procedures of the two groups were the

Table 1 Clinicopathological characteristics of patients ($n = 56$) who underwent total-body PET/CT with half-dose ^{18}F -FDG activity

Characteristic	Value
Age (years old)	63.9 ± 10.0 (range 29–80)
Sex	
Male	38 (67.9%)
Female	18 (32.1%)
BMI (kg/m ²)	22.9 ± 2.7
Diabetes	9 (16.1%)
Blood glucose before injection (mmol/L)	5.7 ± 1.1
Injected dose (MBq)	119.5 ± 18.7
Waiting time (min)	74.5 ± 22.9
Overall stage	
I	18 (32.1%)
II	6 (10.7%)
III	10 (17.9%)
IV	22 (39.3%)
Clinical T stage	
T1	23 (41.1%)
T2	14 (25.0%)
T3	9 (16.0%)
T4	10 (17.9%)
Clinical N stage	
N0	27 (48.2%)
N1	3 (5.4%)
N2	9 (16.1%)
N3	17 (30.3%)
Clinical M stage	
M0	34 (60.7%)
M1	22 (39.3%)
Histology	
Adenocarcinoma	37 (66.1%)
Squamous cell carcinoma	8 (14.3%)
Small-cell carcinoma	4 (7.1%)
Neuroendocrine carcinoma	3 (5.4%)
Mixed/unspecified	4 (7.1%)

same. No significant difference was found between the two groups in terms of age, sex, BMI, history of diabetes, blood glucose level before injection, waiting time, number of lesions in the lung or pathological type of lesions. Table 2 lists all these factors. This study was approved by the Medical Ethics Committee of Zhongshan Hospital Fudan University (2019-029R), and informed consent was obtained from the half-dose group.

PET/CT examination

Patients were required to avoid strenuous exercise within 24 h and to fast for 6 h prior to ^{18}F -FDG PET/CT imaging. At the time of ^{18}F -FDG injection, the fasting blood glucose level was less than 10 mmol/L. The blood glucose level of patients with

diabetes should be controlled below 11.0 mmol/L. In the half-dose group, patients received an injection of ^{18}F -FDG according to their body weight (1.85 MBq/kg). Patients in the full-dose group were also injected intravenously with ^{18}F -FDG according to their body weight (3.7 MBq/kg). ^{18}F -FDG was provided by Shanghai Atom Kexing Pharmaceutical Co., Ltd. and its radiochemical purity was more than 95%. All patients rested quietly for approximately 60 min after the injection of ^{18}F -FDG and then underwent PET/CT imaging.

For the half-dose group, the PET/CT scanner used LYSO crystal and SiPM photoelectric conversion technology with a 194-cm-long longitudinal FOV (uEXPLORER, United Imaging Healthcare, Shanghai, China). The PET/CT scanner used in the full-dose group had a digital light guide device with 112 rings (uM780, United Imaging Healthcare,

Table 2 Clinicopathological characteristics of patients who underwent surgery between the half-dose group and the full-dose group

	Half-dose group underwent surgery (<i>n</i> = 28)	Full-dose group underwent surgery (<i>n</i> = 28)	<i>P</i> value
Age (years)	60.6 ± 11.0	62.5 ± 10.2	0.51
Sex			1.00
Female	10	10	
Male	18	18	
BMI (kg/m ²)	22.6 ± 2.7	22.9 ± 2.7	0.72
Diabetes	4 (14.2%)	2 (7.1%)	0.67
Blood glucose level before injection (mmol/L)	5.4 ± 0.9	5.3 ± 0.9	0.45
Injected dose (MBq)	119.5 ± 18.8	229.8 ± 42.9	< 0.001
Waiting time (min)	69.5 ± 19.2	63.5 ± 19.9	0.20
Overall stage			
I	18	18	1.00
II	6	6	1.00
III	4	4	1.00
Pathological T stage			
T1	18	19	1.00
T2	7	6	1.00
T3	2	2	1.00
T4	1	1	1.00
Pathological N stage			
N0	24	24	1.00
N2	4	4	1.00
Pathological M stage			
M0	28	28	1.00
Number of lesions in the lung (<i>n</i>)	30	30	1.00
Lesion size (mm)	26.0 ± 12.5 (range 10.1 ~ 64.4)	26.3 ± 14.2 (range 7.0 ~ 63.6)	0.80
Intrapulmonary nature of lesions			
Solid lesions (number)	21 (70.0%)	21 (70.0%)	1.00
Ground-glass lesions (number)	9 (30.0%)	9 (30.0%)	1.00
Pathological pattern			
Adenocarcinoma (number)	23 (76.7%)	23 (76.7%)	1.00
Squamous carcinoma (number)	6 (20.0%)	5 (16.7%)	1.00
Other cancer (number)	1 (3.3%)	2 (6.7%)	1.00

Shanghai, China). The comparison of the specifications between the two scanners was shown in Table 3.

Image acquisition and processing

Images in the half-dose group were acquired by a total-body PET/CT scanner using a 3D list-mode, which would continuously perform PET scans for 15 min. The PET images were first reconstructed using all 15 min data and were further split into 4-min and 2-min duration groups to simulate fast acquisition scenarios. To compare these data with the routine clinical PET/CT acquisition with a speed of 2 min/bed, we chose the reconstructed 4-min and 2-min duration images. In the present study, the image series reconstructed with durations of 15 min, 4 min and 2 min were referred to as G15, G4 and G2, respectively. The total-body scanner had a reconstructed spatial resolution of 1 cm from the centre of the field of view [9]. The coincidence time window varied with the unit difference to account for the different path lengths through the body and ranged from 4.5 to 6.9 ns [9]. PET images were reconstructed by the ordered subset expectation maximization (OSEM) algorithm with the following parameters: time of flight (TOF) and point spread function (PSF) modelling, 3 iterations and 20 subsets, matrix 192×192 , slice thickness 1.443 mm and the full width at half maximum of the Gaussian filter function 3 mm. The CT scan parameters were as follows: tube voltage 120 kV, tube current 140 mAs, pitch 1.0, collimation 0.5 mm and reconstructed slice thickness 0.5 mm.

Table 3 Characteristics of the uEXPLORER and uM780 PET/CT systems

PET/CT systems	uEXPLORER	uM780
Crystal material	LYSO	LYSO
Amplifier	SiPM	SiPM
Number of rings	672	112
Size of crystals [mm^3]	$2.76 \times 2.76 \times 18$	$2.76 \times 2.59 \times 18$
Axial FOV [mm]	1940	300
Overlap [%]	/	25
NEMA sensitivity [cps/kBq]	176	15
FWHM axial @ 1 cm [mm]	2.9	2.9
Coincidence window width (ns)	4.5	4
Timing resolution (ps)	430	430
Lower energy threshold (keV)	430	430
Slice thickness [mm]	1.443	1.340
Image planes in the axial FOV	1343	/

FOV field of view, FWHM full width at half maximum, LYSO lutetium-yttrium oxyorthosilicate, NEMA National Electrical Manufacturers Association, PM photomultiplier; SiPM silicon photomultiplier

PET/CT scans in the full-dose group ranged from the roof of the skull to the middle of the femur. The longitudinal field of view was 30 cm, and the scanning speed was 2 min/bed. The PET image reconstruction algorithm used the OSEM iteration (2 iterations, 20 subsets), TOF technology and PSF technology, and the full width at half maximum of the Gaussian filter function was 3 mm. The CT scanning parameters were as follows: tube voltage 120 kV, tube current 140 mAs, pitch 1.0, collimation 0.5 mm and reconstructed slice thickness 0.5 mm.

Analysis of PET/CT imaging

The PET/CT images were independently evaluated by two experienced nuclear radiologists. In cases of discrepancy, an agreement was reached after mutual consultation. According to the Likert quintile [10], the image quality by subjective analysis was as follows: 5, excellent image quality; 4, good image quality; 3, average image quality; 2, poor image quality; and 1, very poor image quality. Image quality scores of 3 or higher were qualified, indicating that the needs of clinical diagnosis could be met, whereas image quality scores of 1–2 did not meet the needs of clinical diagnosis.

The objective image quality analysis was performed by an experienced technician under the supervision of a nuclear radiologist. A 2D circular region of interest (ROI) was placed in a homogeneous area in the right liver lobe and in the ascending aorta at the level of the bronchial bifurcation as the blood pool. Avoiding intrahepatic lesions and large blood vessels, the diameter of the ROI within the right liver lobe was limited to 20 mm. The maximum of the standard uptake value (SUVmax), the mean of the standard uptake value (SUVmean) and the standard deviation (SD) of the ROI in the liver were recorded. The signal-to-noise ratio (SNR) of liver was calculated by dividing the liver SUVmean in the ROI by its SD. The SUVmax and SUVmean in the ascending aorta were recorded. Another ROI was placed to measure the SUVmax of a lung lesion with the maximal diameter on the transverse view. In cases of multiple lung lesions, the lung lesion with the highest SUVmax in each patient was selected in this study. The tumour-to-background ratio (TBR) was calculated by dividing the SUVmax of the lung lesion by the SUVmean of the blood pool. All ROI measurements were taken on G15 images, and then the copy-and-paste ROI function was used to measure the same lesion on the G2 and G4 images to ensure that the location and the size of the ROI were identical across them.

Lesion detectability

All avid FDG lesions confidentially identified by the readers were counted, and the location of the lesion was documented. The result of G15 served as the reference to test the lesion

detectability in G4 and G2. The lesions' detectability was measured by the lesion detection rate in this study.

Statistical analysis

SPSS 19.0 software for Windows (IBM SPSS Inc., Armonk, NY, USA) was used for statistical analysis, with p values < 0.05 indicating a significant difference. Continuous variables were expressed as the mean \pm standard deviation (SD). The Kruskal-Wallis rank-sum test and Dunn's post hoc test for multiple comparisons were used for the comparison of the subjective image quality among the groups. Independent sample t tests and non-parametric Mann-Whitney U tests were used to compare data between the half-dose group and the full-dose group. Paired t tests with Bonferroni correction were used to compare the objective image quality among G15, G4 and G2 images in the half-dose group.

Results

Patient characteristics

In the half-dose group, a total of 56 patients (38 males, 18 females; 63.9 ± 10.0 years old) confirmed to have primary lung cancer were enrolled. The details were listed in Table 1. Compared with the 28 lung cancer patients who underwent surgery in the half-dose group, the 28 lung cancer patients confirmed by surgical pathology who underwent conventional PET/CT scans injected with full-dose (3.70 MBq/kg) ^{18}F -FDG activity were screened. As shown in Table 2, there were no statistically significant differences in age, sex, BMI, history of diabetes, injection and imaging intervals or the diameter, nature and pathological type of the lung lesions between the half-dose group and full-dose group, with $p > 0.05$. The difference in the injection dose was statistically significant, with $p < 0.001$.

Comparison of PET/CT image quality scores

According to the PET/CT image quality scores shown in Table 4, all the image qualities in the full-dose group and

the half-dose group met the clinical diagnosis requirements. Figure 1 showed that the scores were typically evaluated as 4 points for G2 and 5 points for G4 and G15. Based on the results, the frequency of an image quality score evaluated as 5 points in G2 was greater than that in the full-dose group (35.7% vs 7.1%). The image quality score also showed the same tendency between G2 (4.3 ± 0.6) and the full-dose group (3.7 ± 0.6), with a significant difference ($p = 0.004$). In the half-dose group, the mean and SD of the image quality scores of G2, G4 and G15 were 4.3 ± 0.6 , 4.9 ± 0.2 and 5.0 ± 0.0 , respectively. Additionally, 53 cases (94.6%) in G4 and 56 cases in G15 (100%) were evaluated as 5 points. The half-dose group showed a significant difference the image quality score between G2 and G4, with $p < 0.001$, while the difference between G4 and G15 was not significant ($p = 1.0$).

Objective evaluation of PET/CT image quality between the half-dose group and full-dose group

As shown in Table 5, the image quality was compared between G2 (28 cases of surgery) and the full-dose group (28 cases of surgery) by objective analysis. The liver SNR in G2 (11.7 ± 1.5) was significantly higher than that in the full-dose group (8.3 ± 1.2 , $p < 0.001$). In addition, the average SUVmax and SUVmean of the liver in G2 were 3.4 ± 0.5 and 2.7 ± 0.5 , respectively, which were significantly higher than those in the full-dose group (2.9 ± 0.5 and 2.1 ± 0.3 , respectively; $p < 0.001$). The average SUVmax and SUVmean of the blood pool in G2 were 2.5 ± 0.5 and 2.0 ± 0.4 , respectively, which were significantly higher than those of the full-dose group (2.2 ± 0.4 and 1.5 ± 0.2 , respectively) ($p < 0.05$). The mean SUVmax of the lesions and the TBR were not significantly different between G2 (9.2 ± 7.8 , 4.7 ± 3.9) and the full-dose group (8.1 ± 5.7 , 5.4 ± 3.9), with $p = 0.47$ and $p = 0.38$.

Half-dose total-body image quality

The lung lesions were clearly visible on the G2, G4 and G15 images. The liver SNR of G2, G4 and G15 were 11.1 ± 1.7 , 15.2 ± 3.4 and 30.5 ± 6.0 , respectively. The differences were statistically significant (all $p < 0.001$), as shown in Fig. 2a. The average liver SUVmax, liver SUVmean, blood pool

Table 4 Subjective image quality (number and percentage)

	Excellent (score 5)	Good (score 4)	Average (score 3)	Poor (score 2)	Very poor (score 1)	Average score
Full-dose group 2 min/bed ($n = 28$)	2 (7.1%)	15 (53.6%)	11 (39.3%)	0	0	3.7 ± 0.6
G2 ($n = 56$)	20 (35.7%)	33 (58.9%)	3 (5.4%)	0	0	4.3 ± 0.6
G4 ($n = 56$)	53 (94.6%)	3 (5.4%)	0	0	0	4.9 ± 0.2
G15 ($n = 56$)	56 (100%)	0	0	0	0	5.0 ± 0.0

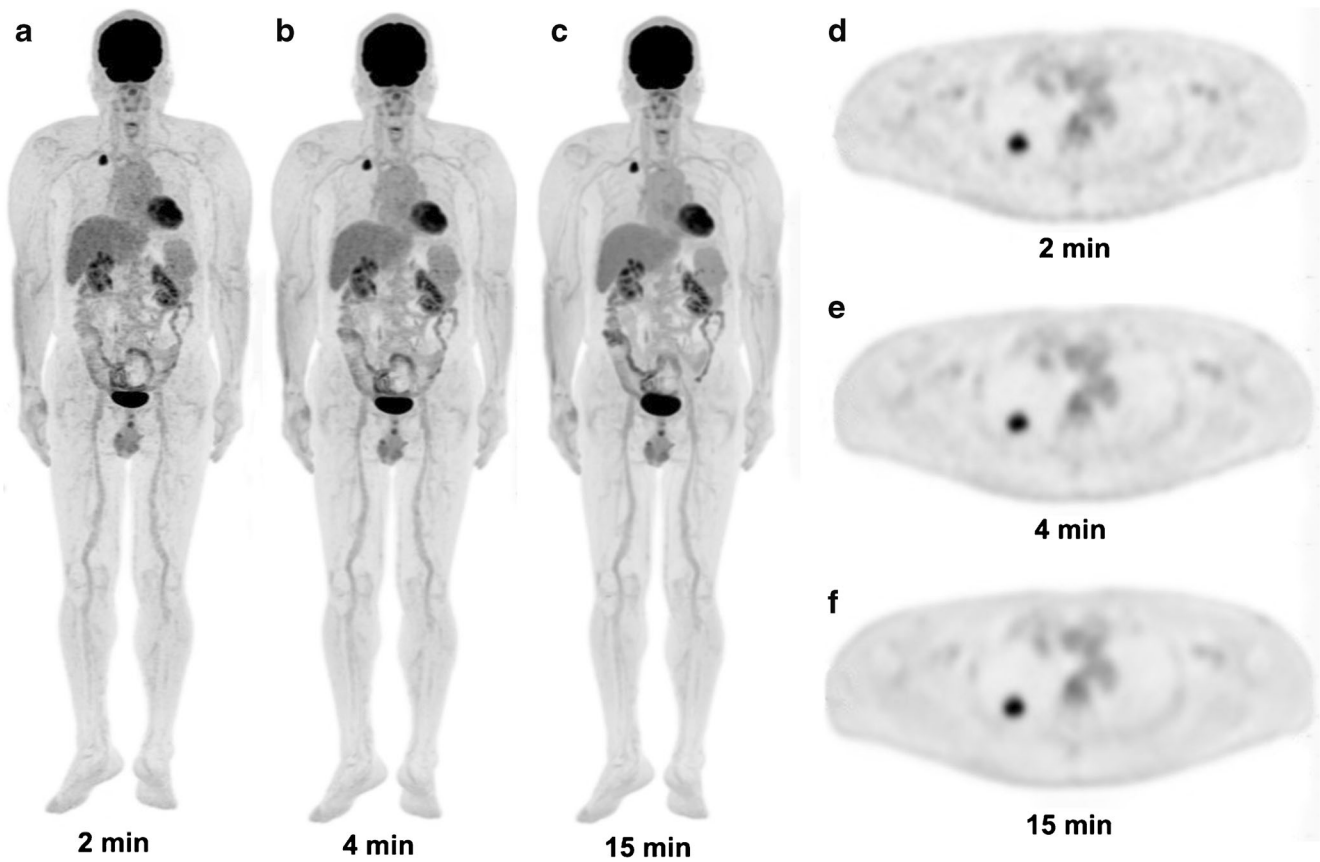


Fig. 1 A 58-year-old man with infiltrating adenocarcinoma of the lung confirmed by surgery. The avid FDG lesions in the upper lobe of the right lung were identified in maximum intensity projection (MIP) (a–c) and axial images (d–f) for G2, G4 and G15. The image quality scores of G2,

G4 and G15 were 4, 5 and 5 points, respectively. The liver SNR were 10.1, 13.0 and 22.9 in G2, G4 and G15, respectively. The lesion SUVmax values of G2, G4 and G15 were 8.1, 7.8 and 7.5, respectively

SUVmax and SUVmean in G2 were 3.3 ± 0.5 , 2.6 ± 0.4 , 2.5 ± 0.4 and 1.9 ± 0.4 , which were greater than those in G4 (3.1 ± 0.5 , 2.6 ± 0.4 , 2.3 ± 0.4 and 1.9 ± 0.4) and G15 (2.9 ± 0.5 , 2.6 ± 0.4 , 2.1 ± 0.4 and 1.8 ± 0.4). The liver SUVmax was significantly different between G2 and G15 ($p < 0.001$) and between G4 and G15 ($p = 0.026$), as shown in Fig. 2a. The blood pool SUVmax between G2 and G15 was significantly different ($p = 0.01$).

The TBR and SUVmax of lung lesions, lymph nodes and bone lesions were almost the same in G2 and G4 and were

greater than those in G15. However, there were no significant differences among G2, G4 and G15, all $p > 0.05$, as shown in Fig. 2b. The SUVmax values of lung lesions in G2, G4 and G15 were 14.8 ± 10.4 , 14.7 ± 10.3 and 13.0 ± 8.7 , respectively, and the corresponding TBR of lung lesions were 8.4 ± 6.9 , 8.4 ± 6.9 and 7.6 ± 5.5 , respectively. The SUVmax values of lymph nodes in G2, G4 and G15 were 15.6 ± 7.0 , 15.4 ± 6.7 and 13.0 ± 5.7 , and the corresponding TBR values of lymph nodes were 9.0 ± 5.4 , 9.0 ± 5.3 and 7.7 ± 4.2 , respectively. The SUVmax values of bone lesions in G2, G4 and G15 were

Table 5 Objective image quality parameters (mean \pm standard deviation) in total-body PET/CT and conventional PET/CT

SUV parameters	G2 group underwent surgery (n = 28)	Full-dose group underwent surgery (n = 28)	P value
Liver SUVmax (range)	3.4 ± 0.5 (2.4~4.3)	2.9 ± 0.5 (1.8~3.6)	<0.001
Liver SUVmean (range)	2.7 ± 0.5 (1.9~3.7)	2.1 ± 0.3 (1.4~2.7)	<0.001
Liver SNR (range)	11.7 ± 1.5 (9.1~14.2)	8.3 ± 1.2 (6.6~10.9)	<0.001
Blood pool SUVmax (range)	2.5 ± 0.5 (1.7~3.4)	2.2 ± 0.4 (1.4~2.8)	0.007
Blood pool SUVmean (range)	2.0 ± 0.4 (1.3~2.8)	1.5 ± 0.2 (1.0~2.0)	<0.001
Lesions SUVmax (range)	9.2 ± 7.8 (1.1~30.8)	8.1 ± 5.7 (1.5~21.1)	0.47
Lung lesions to blood pool SUVratio	4.7 ± 3.9 (0.5~23.7)	5.4 ± 3.9 (1.0~15.7)	0.38

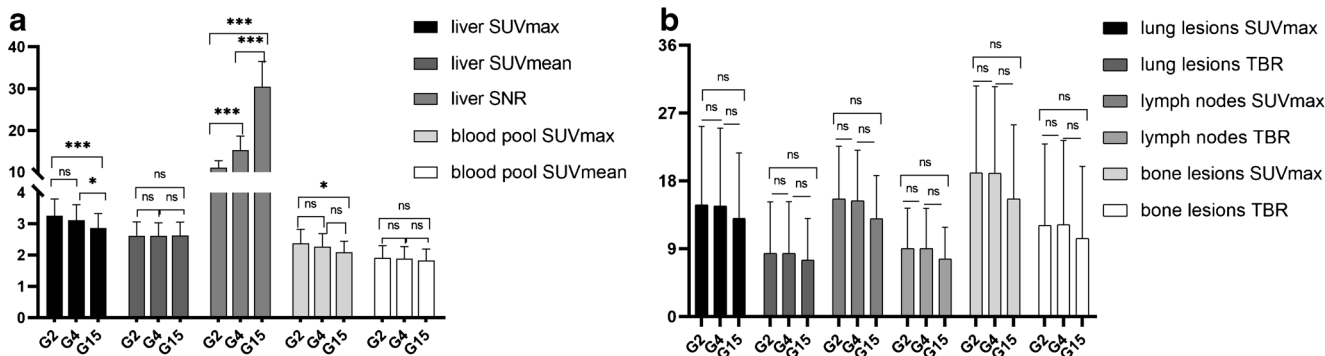


Fig. 2 Comparison of objective image quality parameters in total-body PET/CT among G2, G4 and G15 images. **a** The liver SUVmax, SUVmean and SNR as well as the blood pool SUVmax and SUVmean were compared among G2, G4 and G15. The differences in the liver SNR were statistically significant ($p < 0.001$). The liver SUVmax was significantly different between G2 and G15 ($p < 0.001$) and between G4 and G15 ($p = 0.026$). The blood pool SUVmax was significantly different

between G2 and G15, with $p = 0.01$. **b** The TBR and SUVmax values of lung lesions, lymph nodes and bone lesions were almost the same in G2 and G4 and were greater than those in G15. The differences were not statistically significant among the three groups, all $p > 0.05$. (“*” and “***” indicate $p < 0.05$ and < 0.001 , respectively, while “ns” denotes no significance)

19.1 ± 11.6 , 19.0 ± 11.5 and 15.6 ± 9.8 , and the corresponding TBR values of bone lesions were 12.1 ± 10.8 , 12.2 ± 11.1 and 10.4 ± 9.5 , respectively.

Lesion detectability

On the PET G15 images, 58 primary lung cancer lesions were identified. In G2 and G4, all primary lung cancer lesions (100%) were found. On the PET G15 images, there were 28 cases of lymph node lesions, 16 cases of bone lesions, 4 cases of intrapulmonary metastasis, 4 cases of liver metastasis, 3

cases of adrenal lesions, 2 cases of peritoneal lesions, 1 case of intracranial lesions and one case of diaphragmatic lesions. All these lesions (100%) could be identified in G2 and G4, and a typical case was shown in Fig. 3.

Discussion

The common standardized imaging procedure of ^{18}F -FDG PET/CT will help to promote the appropriate use and increase the value of clinical application. The European Association of

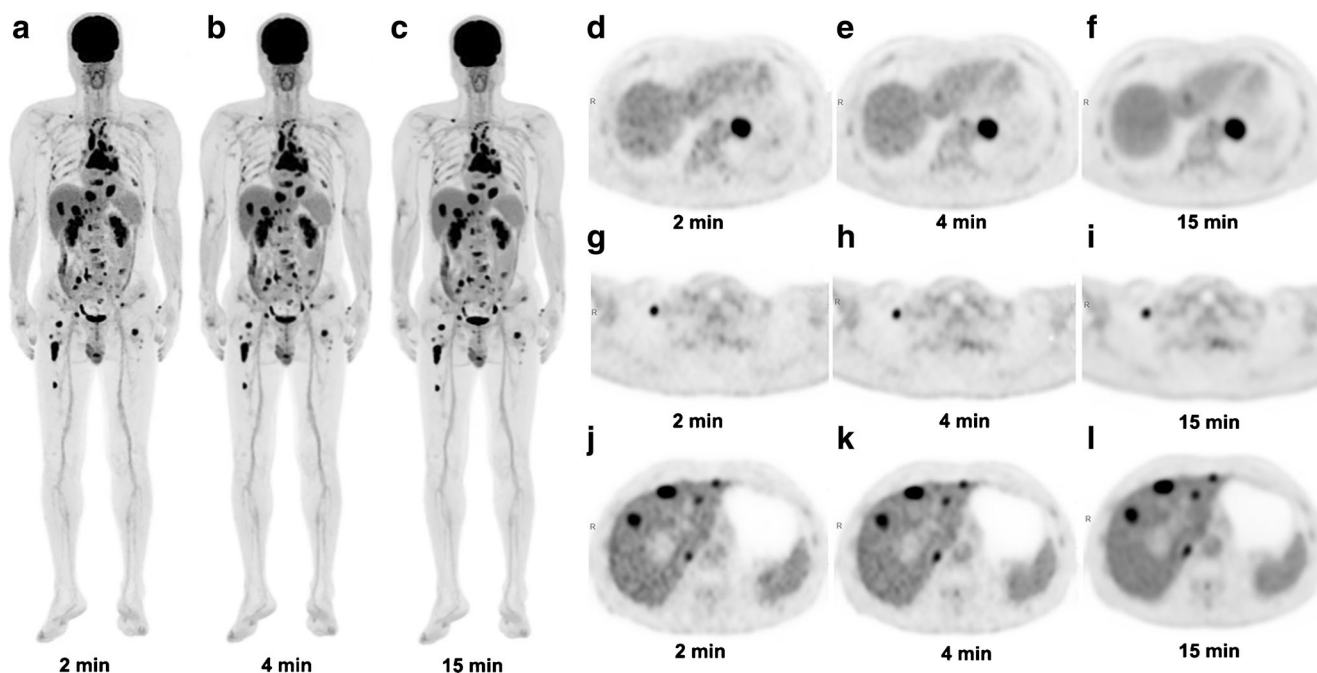


Fig. 3 A 58-year-old man with non-small-cell lung cancer confirmed by bronchoscopy. PET showed avid FDG in multiple lymph nodes (left hilum, mediastinum and right clavicular area), liver, multiple bones and right adrenal gland in MIP (a–c) for G2, G4 and G15. The axial images

showed lesions in the inferior lobe of the left lung (d–f), right clavicular area (g–i), liver and right adrenal gland (j–l) for G2, G4 and G15. The image quality score was 5 points in G2, G4 and G15. The liver SNR were 13.3, 16.7 and 24.8 in G2, G4 and G15, respectively

Nuclear Medicine (EANM) procedure guidelines for tumour imaging with ^{18}F -FDG PET/CT have been amended to keep patient radiation exposure levels as low as reasonably possible with the (ALARA) principles [11]. Recommendations for the ^{18}F -FDG dose and administered activity are usually calculated according to the patient's weight, acquisition time and the sensitivity profile of the PET bed overlap. The current recommended ^{18}F -FDG activity is no less than 7 MBq/kg per minute per bed, which is converted to a data acquisition time of 2 min/bed, and the ^{18}F -FDG dose that is needed for injection into patients is approximately 3.7 MBq/kg [11]. In our department, we employed the EANM procedure guidelines as clinical routine for PET/CT imaging: an injected dose of 3.7 MBq/kg (full-dose) ^{18}F -FDG and a data acquisition time of 2 min/bed. Patients in the half-dose group were injected with 1.85 MBq/kg ^{18}F -FDG and underwent total-body PET/CT imaging. In addition, due to the clinical routine 780 PET/CT acquisition with a speed of 2 min/bed in our centre, we chose the G2 and G4 images for total-body PET/CT to compare with clinical routine PET/CT with half-dose FDG.

The image quality of PET is affected by multiple factors, such as instrument use, imaging parameters, reconstruction parameters, imaging agents, waiting time, subject preparation and individual subject factors (including blood glucose level, history of diabetes, BMI, etc.) [12–16]. Therefore, to reduce interference factors that affect the quality evaluation of PET images as much as possible, all cases in this study were collected during the same period to ensure that the radiochemical purity of ^{18}F -FDG was basically the same. The subject preparation and process of PET/CT imaging were consistent between the half-dose group and the full-dose group. There were no significant differences in age, sex, BMI, history of diabetes, interval time between agent injection and patient imaging or the diameter, nature or pathological type of lung lesions between the two groups. This made the image quality of the two groups with resected lesions more comparable.

With the rapid development of medical imaging equipment, the performance of PET/CT detectors has gradually improved. The total-body PET detector crystals measure $2.76 \times 2.76 \text{ mm}^2$ in cross section by 18.1 mm in depth and are arranged in 7×6 arrays coupled to SiPMs for read-out. The system has 8 axial units, each with an axial FOV of 24 cm and with a gap of just 2.5 mm between units. The total-body PET/CT scanner has the following advantages. First, it possesses an ultralong PET axial FOV of 194 cm. Second, compared with the current commercial PET/CT system, it has ultrahigh sensitivity. A single-bed scan can achieve total body imaging, greatly reducing the scanning time. Otherwise, due to the ultrahigh sensitivity, the image quality can meet the needs of clinical diagnosis at a relatively low tracer dose [17–19]. In this study, our data showed that the image quality of G2 was better than that of the full-dose group. The image quality score in the former group (4.3 ± 0.6) was higher than

that in the full-dose group (3.7 ± 0.6 , $p = 0.004$). The SNR of the half-dose group was also significantly higher than that of the full-dose group ($p < 0.001$). These results suggested that total-body PET/CT with full-dose (1.85 MBq/kg) ^{18}F -FDG was feasible for clinical application, the quality of the PET images could be improved and the dose of radiation to patients could be reduced. In addition, the SUVmax and SUVmean of the liver and blood pool in G2 were higher than those in the full-dose group. This might likely be because total-body PET/CT possesses a 194-cm-long axial FOV, which allows simultaneous recording of coincidence photons from the entire human body and would increase the information obtained by the detector, resulting in an increase in the values of SUVmax and SUVmean in the liver and blood pool. Second, there were individual differences between G2 and the full-dose group, and the number of samples was relatively small.

In terms of the acquisition time, a longer time always results in higher image quality. Taking the G15 image as a reference, the image quality score of G15 was 5.0. The image quality of total-body PET in G2 was slightly inferior to that in G4, but the image quality in the two groups could meet the needs of clinical diagnosis, and lung lesions were also clearly demonstrated. The image quality scores in G2 and G4 were 4.3 ± 0.6 and 4.9 ± 0.2 , respectively ($p < 0.001$). The objective analysed index of liver SNR increased with reconstructed time in G2, G4 and G15. The longer the time, the better the PET image quality was, which is consistent with previous research results [20]. The objective index values of the SUVmax in the liver and blood pool gradually decreased in G2, G4 and G15, which provided an estimation of the deviation in the SUVmax resulting from the noise, as shown in the study by Zhang et al [21] This means that extending the acquisition time could reduce image noise, making the reduction in the SUV values of the liver and blood pool closer to the real value, which is consistent with a previous study by Halpern et al [22] A shortened reconstruction time might affect the precision of the SUV and TBR. In this study, the lesion detection rate was 100% in G2 and G4, in reference to G15. The average SUVmax and TNR values of all lesions in G2 and G4 were higher than those in G15, but with no significant difference ($p > 0.05$). This was similar to the results of Hausmann et al. [23] who reported that the acquisition time had no significant effect on the SUVmax of the lesion. The results suggested that a sufficient and acceptable imaging quality of total-body PET/CT with half-dose ^{18}F -FDG in lung cancer could be achieved in G2.

There were some potential limitations in this study. First, it was a single-centre study, and the relatively small population might have resulted in selection bias. Second, it was still unavoidable that individual differences would affect the quality of PET/CT images because the enrolled cases were different between the half-dose group and the full-dose group. Third, our study only comparatively analysed the PET/CT image

quality of these cases with surgical pathology in G2 and in the full-dose group, did not comparatively analyse the PET/CT image quality of the remaining cases without surgery between the two groups. Fourth, it is well known that CT image features are vital for the diagnosis of lung cancer. Our study mainly focused on the analysis of PET images and not on CT images. Fifth, our study was based on FDG injection protocols, which may not be extrapolated to tracers beyond FDG. Finally, it may be a better choice to use pathological findings as the reference to test lesion detectability rather than referring to the G15 images.

Due to the 194-cm-long FOV, ultrahigh system sensitivity and good spatial resolution, total-body PET could be performed with a low administered activity or short acquisition time, could achieve total-body dynamic acquisition and could provide high detectability for small lesions and distant metastases. We preliminarily explored the feasibility of the clinical application of total-body PET/CT with half-dose FDG in this study. In conclusion, we demonstrated that total-body PET with half-dose ^{18}F -FDG activity for G2 and G4 images could achieve a comparable image quality to conventional PET, and the image quality was even superior to that of conventional PET. This result suggested that the injected dose could be reduced, which would help to reduce radiation doses for subjects.

Authors' contributions Hui Tan and Xiuli Sui were involved in the study design, data analysis and manuscript preparation. Hongyan Yin and Wujian Mao helped with data processing. Haojun Yu, Yusen Gu and Shuguang Chen helped with image acquisition and processing. Pengcheng Hu helped with the revision of the manuscript. Hongcheng Shi designed the study and contributed to the data analysis and writing of the manuscript. All authors discussed the results and commented on the manuscript.

Funding This study is supported by the National Science Foundation for Scholars of China (Grant No. 81871407 to Hongcheng Shi and Grant No. 81901796 to Hui Tan), the Shanghai Sailing Program Supported by Shanghai Science and Technology Commission (No. 19YF1408300 to Hui Tan) and Shanghai Municipal Key Clinical Specialty (No. shslczdzk03401), Three-year Action Plan of Clinical Skills and Innovation of Shanghai Hospital Development Center (No. SHDC2020CR3079B to Hongcheng Shi), and the Shanghai Science and Technology Committee (No. 20DZ2201800).

Data availability The data that support the findings of this study are available from the corresponding author upon reasonable request.

Compliance with ethical standards

This study was approved by the Medical Ethics Committee of Zhongshan Hospital Fudan University (2019-029R), and informed consent was obtained from the half-dose group.

Conflict of interest The authors declare that they have no conflicts of interest.

Ethical approval All procedures performed in studies involving human participants were in accordance with the ethical standards of the

institutional and/or national research committee and with the 1964 Helsinki declaration and its later amendments or comparable ethical standards.

References

- Kandathil A, Kay FU, Butt YM, Wachsmann JW, Subramaniam RM. Role of FDG PET/CT in the eighth edition of TNM staging of non-small cell lung cancer. *Radiographics*. 2018;38:2134–49.
- Volpi S, Ali JM, Tasker A, Peryt A, Aresu G, Coonar AS. The role of positron emission tomography in the diagnosis, staging and response assessment of non-small cell lung cancer. *Ann Transl Med*. 2018;6(5):95.
- Chen Z, Jiang S, Li Z, Rao L, Zhang X. Clinical value of ^{18}F -FDG PET/CT in prediction of visceral pleural invasion of subsolid nodule stage I lung adenocarcinoma. *Acad Radiol*. 2020. <https://doi.org/10.1016/j.acra.2020.01.019>.
- Doğan C, Fidan A, Cömert SŞ, Kiral N, Salepci B, Parmaksız ET, et al. Can PET-CT predict diagnostic success in ultrasonography-guided transthoracic fine needle aspiration biopsies in lung cancers? *Pulmonology*. 2020. <https://doi.org/10.1016/j.pulmoe.2019.12.005>.
- Nestle U, Schimek-Jasch T, Kremp S, Schaefer-Schuler A, Mix M, Küsters A, et al. Imaging-based target volume reduction in chemoradiotherapy for locally advanced non-small-cell lung cancer (PET-plan): a multicentre, open-label, randomised, controlled trial. *Lancet Oncol*. 2020;21(4):581–92.
- Nutt R. The history of positron emission tomography. *Mol Imaging Biol*. 2002;4(1):11–26.
- Cherry SR, Jones T, Karp JS, Qi J, Moses WW, Badawi RD. Total-body PET: maximizing sensitivity to create new opportunities for clinical research and patient care. *J Nucl Med*. 2018;59(1):3–12.
- Karp JS, Viswanath V, Geagan MJ, Muehllehner G, Pantel AR, Parma MJ, et al. PennPET explorer: design and preliminary performance of a whole-body imager. *J Nucl Med*. 2020;61(1):136–43.
- Badawi RD, Shi H, Hu P, Chen S, Xu T, Price PM, et al. First human imaging studies with the EXPLORER total-body PET scanner. *J Nucl Med*. 2019;60(3):299–303.
- van Sluis J, Boellaard R, Somasundaram A, van Snick P, Borra R, Dierckx R, et al. Image quality and semiquantitative measurements on the biograph vision PET/CT system: initial experiences and comparison with the biograph mCT. *J Nucl Med*. 2020;61(1):129–35.
- Boellaard R, Delgado-Bolton R, Oyen WJ, Giammarile F, Tatsch K, Eschner W, et al. FDG PET/CT: EANM procedure guidelines for tumour imaging: version 2.0. *Eur J Nucl Med Mol Imaging*. 2015;42(2):328–54.
- Büsing KA, Schönberg SO, Brade J, Wasser K. Impact of blood glucose, diabetes, insulin, and obesity on standardized uptake values in tumors and healthy organs on ^{18}F -FDG PET/CT. *Nucl Med Biol*. 2013;40(2):206–13.
- Hadi M, Bacharach SL, Whatley M, Libutti SK, Straus SE, Rao VK, et al. Glucose and insulin variations in patients during the time course of a FDG-PET study and implications for the “glucose-corrected” SUV. *Nucl Med Biol*. 2008;35(4):441–5.
- Cook GJ, Wegner EA, Fogelman I. Pitfalls and artifacts in ^{18}F FDG PET and PET/CT oncologic imaging. *Semin Nucl Med*. 2004;34(2):122–33.
- Cheran SK, Nielsen ND, Patz EF Jr. False-negative findings for primary lung tumors on FDG positron emission tomography: staging and prognostic implications. *Am J Roentgenol*. 2004;182(5):1129–32.

16. Asad S, Aquino SL, Piyavisetpat N, Fischman AJ. False-positive FDG positron emission tomography uptake in nonmalignant chest abnormalities. *Am J Roentgenol.* 2004;182(4):983–9.
17. Pantel AR, Viswanath V, Daube-Witherspoon ME, Dubroff JG, Muehlelehner G, Parma MJ, et al. PennPET explorer: human imaging on a whole-body imager. *J Nucl Med.* 2020;61(1):144–51.
18. Zhang X, Cherry SR, Xie Z, Shi H, Badawi RD, Qi J. Subsecond total-body imaging using ultrasensitive positron emission tomography. *Proc Natl Acad Sci U S A.* 2020;117(5):2265–7.
19. Zhang X, Xie Z, Berg E, Judenhofer MS, Liu W, Xu T, et al. Total-body dynamic reconstruction and parametric imaging on the uEXPLORER. *J Nucl Med.* 2020;61(2):285–91.
20. Akamatsu G, Ishikawa K, Mitsumoto K, Taniguchi T, Ohya N, Baba S, et al. Improvement in PET/CT image quality with a combination of point-spread function and time-of-flight in relation to reconstruction parameters. *J Nucl Med.* 2012;53(11):1716–22.
21. Zhang YQ, Hu PC, Wu RZ, Gu YS, Chen SG, Yu HJ, et al. The image quality, lesion detectability, and acquisition time of (18)F-FDG total-body PET/CT in oncological patients. *Eur J Nucl Med Mol Imaging.* 2020. <https://doi.org/10.1007/s00259-020-04823-w>.
22. Halpern BS, Dahlbom M, Quon A, Schiepers C, Waldherr C, Silverman DH, et al. Impact of patient weight and emission scan duration on PET/CT image quality and lesion detectability. *J Nucl Med.* 2004;45(5):797–801.
23. Hausmann D, Dinter DJ, Sadick M, Brade J, Schoenberg SO, Büsing K. The impact of acquisition time on image quality in whole-body ¹⁸F-FDG PET/CT for cancer staging. *J Nucl Med Technol.* 2012;40(4):255–8.

Publisher's note Springer Nature remains neutral with regard to jurisdictional claims in published maps and institutional affiliations.